Yasuyoshi Yokokohji
Nobuhiko Muramori
Yuji Sato
Tsuneo Yoshikawa

Department of Mechanical Engineering
Graduate School of Engineering
Kyoto University
Kyoto 606-8501, Japan
yokokoji@mech.kyoto-u.ac.jp
http://mech-server.mech.kyoto-u.ac.jp/yoshikawa/

Designing an Encountered-type Haptic Display for Multiple Fingertip Contacts Based on the Observation of Human Grasping Behaviors

Abstract

Unlike conventional haptic devices, an encountered-type device is not held by a user all the time. Instead, the device remains at the location of a virtual object and waits for the user to encounter it. In this paper, we extend this concept to fingertip contacts and design an encountered-type haptic display for multiple fingertip contacts to simulate tasks of grasping an object with any shape and size. Before designing the device, we intensively observed human grasping behaviors. This observation was very helpful to determine the mechanism of the device. An encountered-type device for three-fingered grasping was actually prototyped based on our design.

KEY WORDS—haptic interface, grasping encountered-type, fingertip contact, observation of human motion

1. Introduction

An encountered-type haptic device was first proposed by McNeely (1993). Tachi et al. (1994) proposed a similar idea independently. Unlike conventional haptic devices, an encountered-type device is not held by a user all the time. Instead, the device remains at the location of a virtual object and waits for the user to encounter it. Therefore, encountered-type haptic rendering can provide real free and real touch sensations to the user. Figure 1 illustrates the concept of encountered-type haptic device.

The International Journal of Robotics Research
Vol. 24, No. 9, September 2005, pp. 717-729,
DOI: 10.1177/0278364905057123

The encountered-type approach has been used for two different cases: (i) rendering a single object or multiple objects where the accessible portion is limited (e.g., knobs of doors, hand grips of tools and switches of control panels; Gruenbaum et al. 1997; Yokokohji, Hollis, and Kanade 1999); (ii) rendering a large object by approximating a local region by a set of surface patches (shape approximation device or SAD; Tachi et al. 1994, 1995). We also proposed a path-planning algorithm for encountered-type haptic devices that render multiple virtual objects arbitrarily located in three-dimensional (3D) space (Yokokohji, Kinoshita, and Yoshikawa 2001). As an implementation example, we developed a virtual control panel for automobiles to check the accessibility of switches on the panel in a early design stage. Figure 2 shows our prototyped system.

It would be challenging to extend this concept to simulate grasping an object by multiple fingers as shown in Figure 3. If we prepare small surface patches in such a way that each fingertip of the user's hand can encounter one of these patches, one can simulate tasks of grasping an object with any shape and any size. It should be noted that no matter what the shape of the grasped object is and no matter how large the size of the grasped object is, the position of each fingertip is limited within the working volume of each finger. This fact encourages us to design a device as shown in Figure 3. Actually, Hoshino, Maeda, and Tachi (1997) tried to develop such a device for two-fingered grasping. However, their development was discontinued for some reason. Without careful consideration of the device design, the developed device may not be able to simulate grasping an object with any shape and size as we wanted.

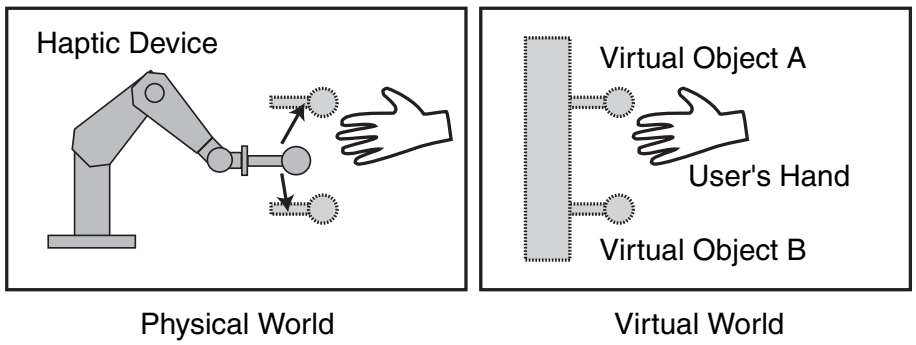

Fig. 1. Concept of the encountered-type haptic device.

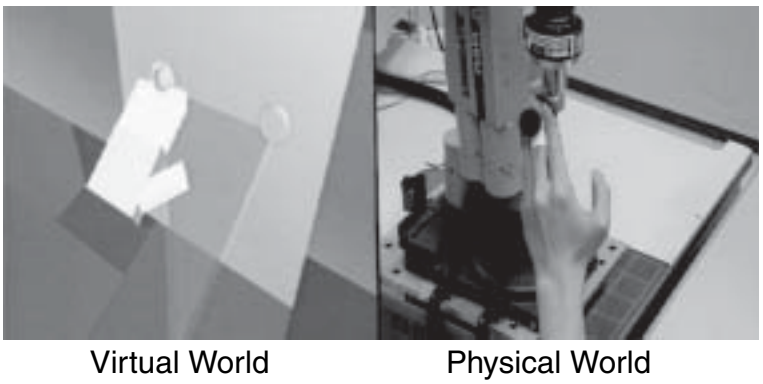

Fig. 2. Prototype of the virtual control panel system.

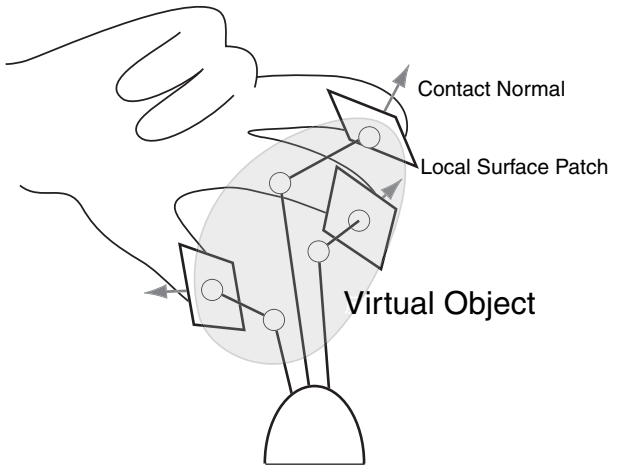

Fig. 3. Local surface patches for simulating fingertip contact.

In this paper, we design an encountered-type haptic display for multiple fingertip contacts to simulate the task of grasping an object with any shape and size. Before designing the device, we intensively observed human grasping behaviors. This observation was very helpful to determine the mechanism of the device. An encountered-type device for three-fingered grasping was actually prototyped based on our design.

2. Basic Design of the Device

2.1. Targeted Grasping Mode

As shown in Figure 4, Napier (1997) classified two major grasping modes: power grasp and precision grasp. Power grasp is used when we grasp a large object or want to apply a large force to the object, having a large contact area between the hand and the object. Precision grasp is used when we grasp a small object or want to manipulate the object in a dextrous manner, having a small contact area at each fingertip. Based on the fundamental classification by Napier, Cutkosky (1989) carried out further classification and developed a hierarchical taxonomy of grasping.

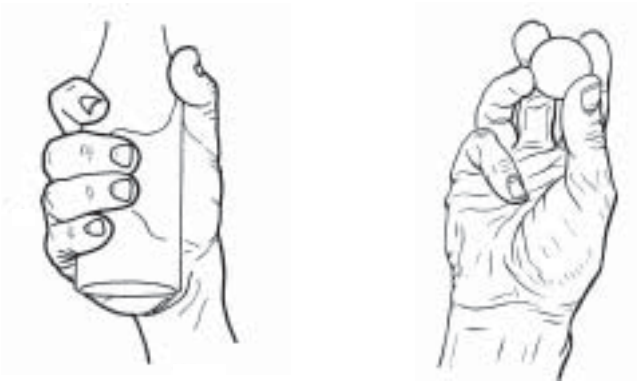

(a) (b)

Fig. 4. Grasping modes (Kapandji 1982): (a) power grasp; (b) precision grasp.

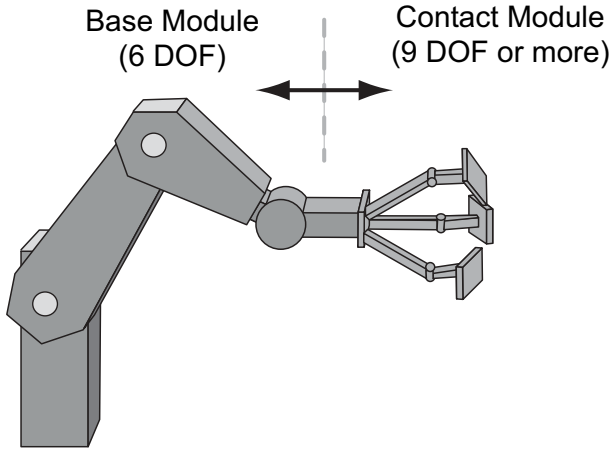

Fig. 5. Arrangement of DOF of the device.

To simulate power grasp, we have to prepare many surface patches to cover a large contact area including not only fingertips but also the palm and middle links of the fingers. It is possible to simulate precision grasp by preparing surface patches only for fingertip contacts. If we exclude power grasp from our target tasks, the device design becomes much easier than considering both modes. In this paper, we design a device for only precision grasp with the thumb, index, and middle fingers.

2.2. Arrangement of Degrees of Freedom

To place a local surface patch anywhere in 3D space, we need five degrees of freedom (DOF). Therefore, 15 is the minimum number of DOF for displaying three surface patches for the thumb, index, and middle fingers. Although we have many possibilities to arrange these 15 DOF, we suppose a configuration shown in Figure 5 where the device can be separated into two modules: the base module and the contact module.

The base module is a serial manipulator and it carries the contact module including three surface patches. We can use a conventional 6-DOF manipulator as the base module. Assigning six DOF to the base module is reasonable, because once the user grasps a rigid object, we can lock all joints of the contact module and control only the base module to simulate object manipulations. Hereafter, we focus on designing the contact module, which should have no less than nine DOF.

3. Related Works

3.1. Encountered-type Haptic Devices and Similar Approaches

As mentioned in Section 1, an encountered-type haptic device was first proposed by McNeely (1993) and Tachi et al. (1994). The authors have been developing encountered-type haptic devices, such as a WYSIWYF display (Yokokohji, Hollis, and Kanade 1999) and a virtual control panel (Yokokohji, Kinoshita, and Yoshikawa 2001).

Hirota and Hirose (1993, 1998) developed a partial surface display system, where a small surface patch or a spherical surface around the fingertip is presented at the location of a virtual object so that the user's fingertip can touch this surface at an appropriate location. Yoshikawa and Nagura (2001) also developed a similar device using a ring-shaped device head and optical sensors to track the user's fingertip. These partial surface display approaches are similar to the encountered-type approach in the sense that it provides actual touch sensations. Since the user's fingertip is always tracked by the device, there is no path-planning problem. However, this advantage induces a drawback of this approach, i.e., the user cannot move his fingertip beyond the working volume of the device. Hirota and Hirose (1995) also extended their approach to presenting an arbitrary shaped surface patch by using a 4×4 array of linear sliding mechanisms.

Iwata, Yano, and Nakaizumi (2001) developed a locomotion interface called the "Gait Master". Two motion platforms are mounted on a turntable and each platform traces human foot motion by string sensors. According to the model of the terrain surface, the platform waits for the user's foot at an appropriate location and supports it during the supporting phase of walking. Therefore, it is a type of encountered-type haptic interface.

3.2. Haptic Devices for Multifingered Grasping

Yoshikawa and Yoshimoto (2000) conducted two-fingered assembly simulation by using two 3-DOF haptic devices. Barbagli, Salisbury, and Devengenzo (2003) developed a device for multifingered grasping by adding an additional

mechanism to the tip of the PHANTOM haptic device. They also considered a haptic rendering algorithm for soft-finger contact.

Kawasaki et al. (2004) developed a multifingered haptic device using a multifingered robotic hand. Each fingertip of a user is connected to the corresponding fingertip of the device via a passive spherical joint. The device can apply 3D force to each fingertip independently. However, since the user's fingertips are always connected to the device, it cannot provide actual free/touch sensations and limits the user's working volume.

To render torsional friction for soft-finger contact by conventional approaches, one needs to implement many actuators to the device so that force and moment can be applied to each fingertip of the user. The encountered-type approach can solve this problem in a relatively simple manner. As mentioned in Section 2.2, if the device has a 6-DOF base module, it is easy to present torsional friction by locking all degrees of freedom of the contact module and moving the base module. It should be noted, however, that the friction properties are governed by the actual friction between the surface patch and the fingertip.

As pointed out by Hirota and Hirose (1993), the partial surface display approach has a potential to render surface textures as well as different frictions by introducing additional mechanisms to the surface patch.

3.3. Human Observation

Human demonstration has been used for programming robot motions. Ikeuchi and Suehoro (1994) and Kuniyoshi, Inaba, and Inoue (1994) performed some pioneering works on this topic. However, they did not focus on designing a robot or a device based on human motion observation.

Kaneko, Tanaka, and Tsuji (1996) proposed scale-dependent enveloping grasp based on the observation of human grasping behavior. They observed human subjects who grasp a cylindrical object with various sizes. Based on this observation, they found that the human grasping strategies can be classified into three patterns according to the size of the object. Inspired by these human grasping strategies, they implemented a similar grasping procedure on their three-fingered robot hand (Kaneko, Tanaka, and Tsuji 1997). Again, they used human behavior just for developing the grasping strategies.

One of the pioneering works concerning robotic hand design based on the intensive observation of human grasping and manipulation is that by Cutkosky (1989). Based on the detailed taxonomy of manufacturing grasp, he suggested the design of versatile robotic hands for manufacturing.

Saito and Nagata (1999) classified and described grasping and manipulation in different ways. They first classified three basic functions of grasping, supporting, pressing, and wrapping. Based on their classification, they described several grasps performed by humans. They also described manipulation as a combination of primitive grasps. They picked up four different types of tasks and designed a hand mechanism that can perform all of these tasks based on their classification and description method (Saito and Nagata 2001). It is interesting that the robot hand designed by them has a completely different structure from a human hand and it is an example of "minimalism" proposed by Bicchi (2000).

In the area of neuro-psychology, it is common to observe human behaviors in various controlled situations in order to analyze the neuro-psychological activities of human. For example, Johansson and his colleagues carried out much work in observing human manipulation and grasping movements (Jenmalm, Goodwin, and Johansson 1998; Burstedt, Flanagan, and Johansson 1999; Jenmalm 2000; Johansson et al. 2001). Of course, they did not intend to design any robotic hand or haptic device based on their observation.

4. Observation of Human Grasping Behavior

4.1. Purpose and Method

In Section 2.2, we considered the arrangement of DOF of the device and determined the necessary DOF for the contact module. However, we did not consider what mechanism is appropriate for the purpose of the contact module. The mechanism should be as simple as possible, with nine DOF if possible. To determine a good mechanism, we must know where each surface patch should be displayed when simulating object grasping. Since the simulated object could be any shape and any size, we must know the grasping behavior of humans with various objects.

For the above reason, we decided to observe human grasping behavior by measuring contact point locations and the direction of contact normals on various objects, which are used in our daily life. Table 1 shows the list of the 50 selected objects.

Figure 6(d) shows a posture measurement device made from a paper bowl. This low-tech device has three joints corresponding to roll–pitch–yaw angles. The device actually has only two joints and the first DOF is the relative rotation angle (ϕ in Figure 6(d)) between the device and the supporting floor. A coordinate frame model is attached at the end of this device as a reference when measuring the orientation of a target coordinate frame. One can move each of these joints manually so that the orientation of the reference coordinate frame model coincides with that of the target coordinate frame and can measure the orientation of a target coordinate frame in roll–pitch–yaw angles by just measuring the angle of each joint of the device by the eye. Since the second joint motion range is limited, we cannot arbitrarily change the orientation of the reference coordinate frame model on the device. In such a case, we have to manage the initial position of the first joint accordingly.

The device is also used for measuring the direction of contact normals. In this case, one can move only the first two

Table 1. List of Grasped Objects

1. Pencil	2. Ball pen	3. Scissors
4. Spoon	5. Toothbrush	6. Pencil case
7. Stick-type paste	8. Eraser	9. File
10. Magnet	11. Bitter orange	12. Book stand
13. Lid of Japanese tea pot	14. Gum tape	15. Deep dish
16. Canned coffee	17. PET bottle (1.5 liter)	18. Kitchen knife
19. Phillips-head screwdriver	20. Scotch tape	21. Tea bowl
22. Portable radio	23. Floppy disk case	24. Pot stand
25. Tissue box	26. Paper cup	27. Cellular phone
28. MD case	29. Clothes hanger	30. Hardcover book
31. Pan	32. Lid of pan	33. Pot plant
34. Plastic tape	35. Grip of umbrella	36. CD case
37. AD converter	38. Extension outlet	39. Trash bin
40. CD player	41. MD player	42. Mouse
43. Battery charger for cellular phone	44. Dictionary	45. Milk carton
46. PET bottle (500 ml)	47. Battery case for notebook PC	48. Underlay
49. Chopstick	50. Bottle of fertilizer supplement for plants	

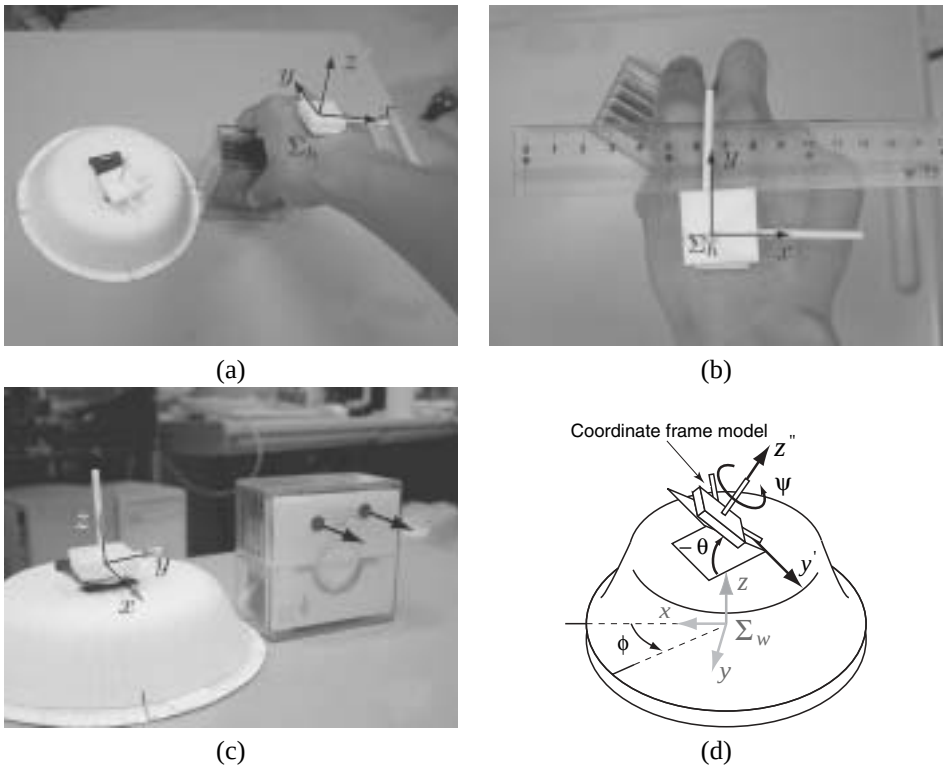

Fig. 6. Posture measurement procedure: (a) step 1; (b) step 2; (c) step 3; (d) posture measurement device.

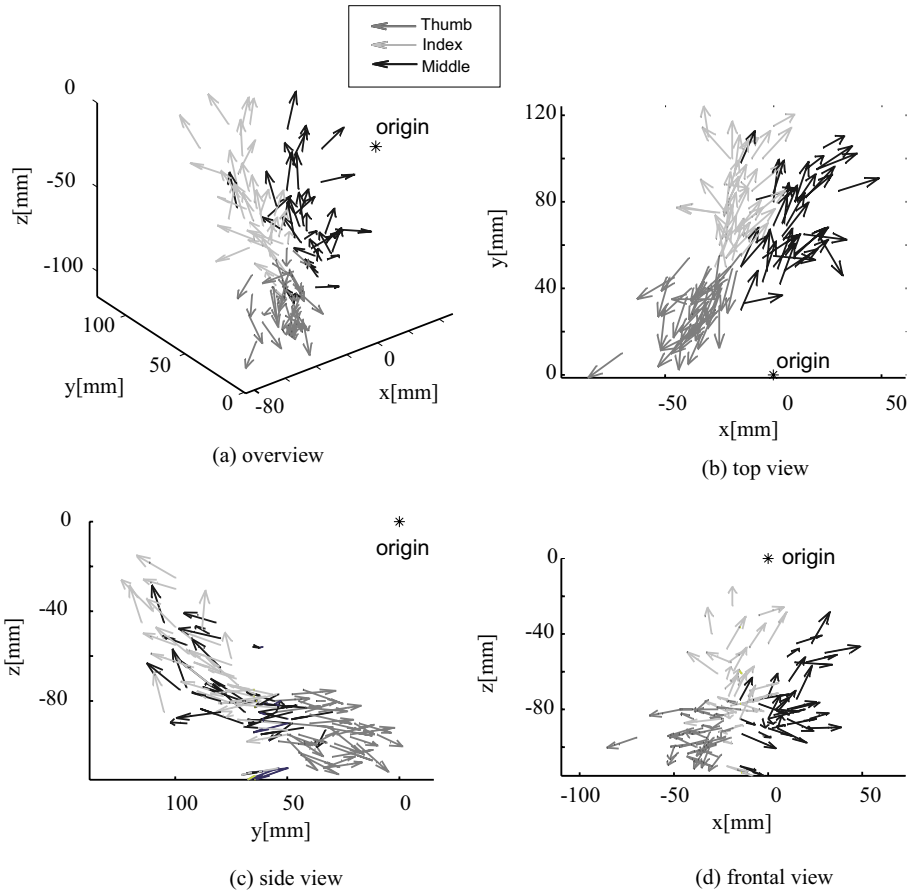

Fig. 7. Contact profiles with respect to Σ_h.

joints of the device so that the direction of the z-axis of the reference coordinate frame model coincides with that of the target contact normal.

Figures 6(a)–(c) illustrate the procedure of the measurement. The actual measurement procedures are explained as follows.

STEP 1. First, we measure the orientation of the hand coordinate frame Σ_h, which is attached to the back of the hand as shown in Figure 6(a), when a human subject grasps an object. This measurement is taken by adjusting the three joints of the low-tech device so that the frame model on the low-tech device and the frame model on the human hand, which represents Σ_h, have the same orientation.

STEP 2. Next, we measure three contact point locations with respect to Σ_h. This measurement is taken by manually placing a rule three times parallel to the x-, y- and z-axes of Σ_h for each contact point.

STEP 3. Finally, we measure the direction of contact normal of each contact point. This measurement is taken by adjusting the first two joints of the low-tech device so that the z-axis of the frame model on the low-tech device and the contact normal vector have the same direction. To identify the contact normals easily, small circular markers are put at the location of the contact points, as shown in Figure 6(c).

Since the above measurements are taken by eye, they are not very accurate. The measurement errors could be up to 10° for the angle and 10 mm for the position. Of course, using a data glove and a magnetic tracker (if we had it) would be much easier and more accurate than this low-tech method. However, we think that the accuracy of this measurement is sufficient for the purpose of designing the basic mechanism of the device.

4.2. Result of the Measurement

Figure 7 shows the result of the measurement. The starting point of each vector corresponds to the contact position with respect to the hand coordinate frame Σ_h. The direction of each vector shows the contact normal direction. Gray vectors

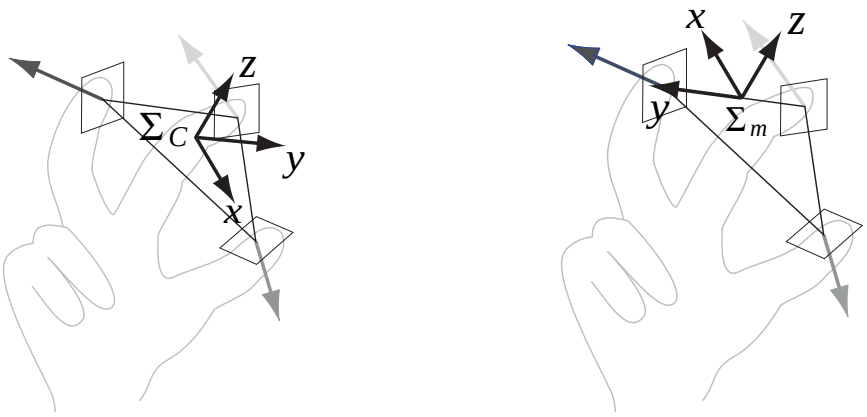

(a) (b)

Fig. 8. Reference coordinate frames: (a) center-of-triangle frame Σ_C; (b) mid-point frame Σ_m.

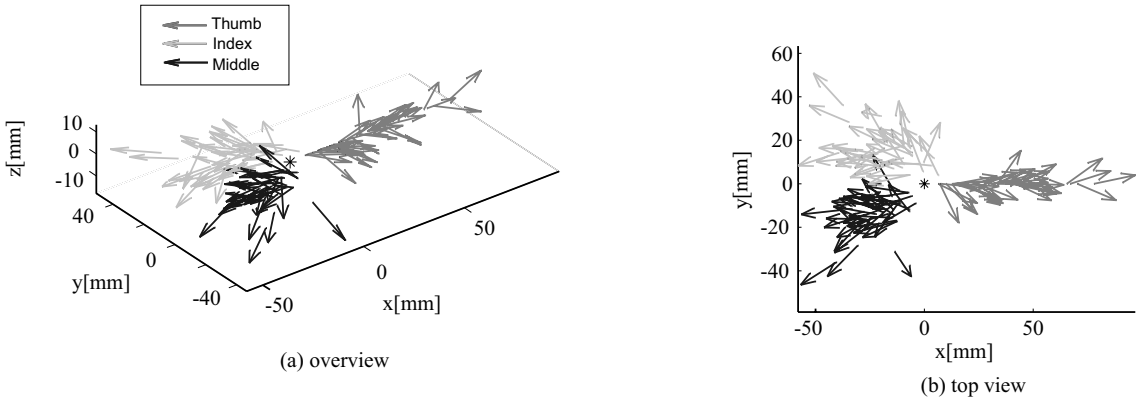

Fig. 9. Contact profiles from Σ_C.

are for the thumb, thin gray vectors are for the index finger, and black vectors are for the middle finger. From Figure 7, especially Figure 7(c), we can see that fingertip positions are distributed on a sphere whose center is located at the origin of Σ_h.

5. Design of the Contact Module

5.1. Examination of the Mechanism

The obtained result can be examined from various points of view by setting the appropriate reference coordinate frames.

The gravity center of the contact-point triangle would be a good candidate for the reference point. We first set a reference frame, called the center-of-triangle frame Σ_C, whose origin is located at the gravity center of the triangle, as shown in Figure 8(a). Figure 9 illustrates the grasping profile viewed from Σ_C. Again, gray vectors are for the thumb, thin gray vectors are for the index finger, and black vectors are for the middle finger. A possible mechanism corresponding to this view is shown in Figure 10 (we call it type A). Two overlapped circles represent a 2-DOF mechanism to change the orientation of the surface patch called the "plate module". The corresponding mechanism has 11 DOF, which is larger than the minimum number of DOF.

Looking at Figure 9, we can see that the index finger and middle finger are distributed symmetrically about the x-axis. Considering this fact, we decided to set a new reference frame, called the mid-point frame Σ_m, whose origin is located at the middle point of two contact points by the index and middle fingers, as shown in Figure 8(b). Figure 11 illustrates the grasping profile viewed from Σ_m. A possible mechanism

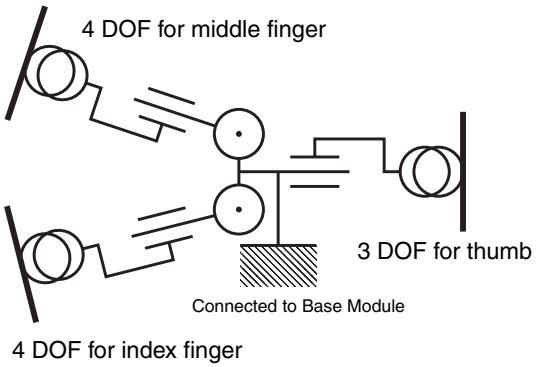

Fig. 10. Structure based on Σ_C (type A).

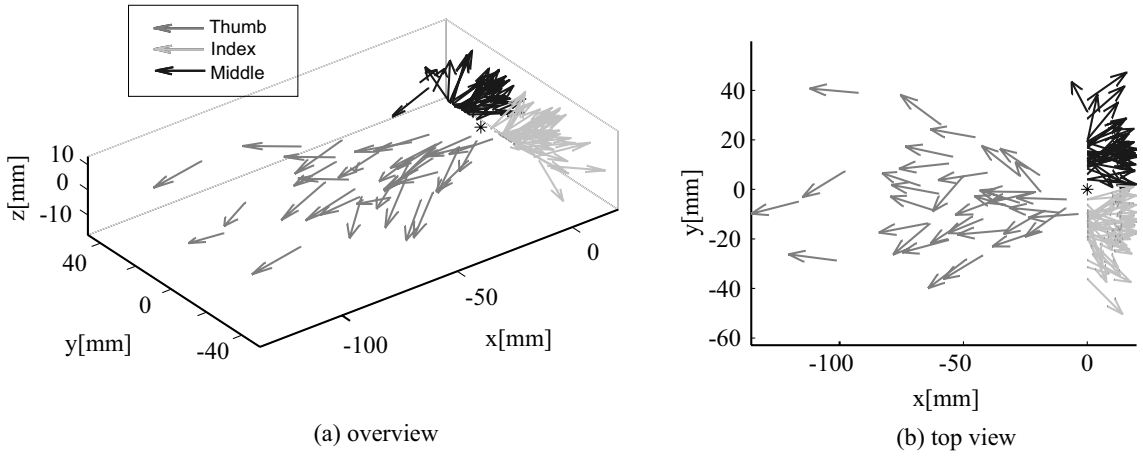

(a) overview (b) top view

Fig. 11. Contact profiles from Σ_m.

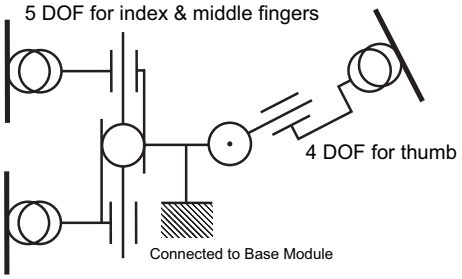

Fig. 12. Structure based on Σ_m (type B).

corresponding to this view is shown in Figure 12 (we call it type B).

Comparing the two mechanisms (type A and type B) shown in Figures 10 and 12, we chose type B as the basic mechanism design of the device for the following reasons. First, type B has nine DOF, the minimum number of DOF for the contact module, while type A has 11 DOF. Secondly, the contact module for the thumb of type B has higher mobility than that of type A and it corresponds well to the anatomical property of the human hand, i.e., our thumb has a wider motion range than the index and middle fingers.

5.2. Plate Module Design

The plate module is a 2-DOF mechanism to change the orientation of the surface patch. From the measured data, we extracted the required motion range of the plate module. Figure 13 illustrates the definition of two angles to determine the direction of contact normal. Table 2 summarizes the angle data. The range of each angle is equal to $\pm 2\sigma$, where σ is the standard deviation of the sampled angles. Assuming a Gaussian distribution, this range covers about 95% populations. We can see that there is no significant difference of motion range between type A and type B. Figure 14(a) illustrates an example of the plate module design that matches the requirement of motion range shown in Table 2.

Table 2. Required Plate Angles

	Type A			Type B		
	Thumb	Index Finger	Middle Finger	Thumb	Index Finger	Middle Finger
Ave(ϕ) (°)	−9	31	−34	−9	−15	15
$\sigma(\phi)$ (°)	25	32	33	25	31	31
Range of ϕ (°)	±50	±64	±66	±50	±62	±62
Ave(θ) (°)	−9	3	6	−9	3	6
$\sigma(\theta)$ (°)	17	20	20	17	20	20
Range of θ (°)	±34	±40	±40	±34	±40	±40

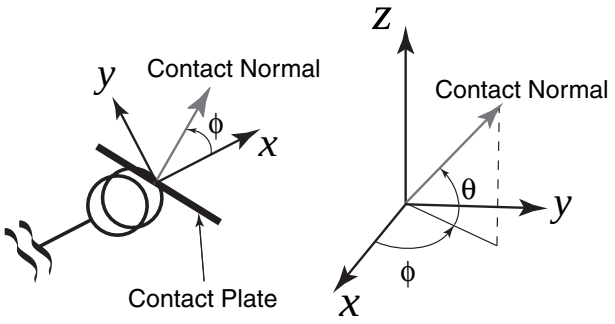

Fig. 13. Definition of plate angles.

(a) (b)

Fig. 14. Initial designs of (a) the plate module and (b) the contact module.

5.3. Prototyping a Contact Module

We proceeded with a further detailed design of the device. Figure 14(b) illustrates an initial design of the contact module. Figure 15(a) illustrates the final design of the contact module by 3D CAD. Then, we actually prototyped a device based on our design. Figure 15(b) shows an overview of the prototyped contact module.

The diameter of the circular surface patch is 30 mm. The orientation of each surface patch is controlled by two DC motors (MAXON RE13EB 2.5W) via a worm gear (reduction ratio 20:1) for pitch (horizontal axis, θ in Figure 13) angle and a built-in gear head (reduction ratio 67:1) for yaw (vertical axis, ϕ in Figure 13) angle. Plate modules for the index and middle fingers are driven by an identical DC motor (MAXON RE13EB 2.5W) with a built-in gear head (reduction ratio 4.1:1) via a ball screw with a 1 mm lead. Since the direction of the screw is reversed in the middle of the shaft, we can open and close these two contact modules using a single motor. Finally, the contact module for the thumb is driven by two DC motors (again both are MAXON RE13EB 2.5W), one with a built-in gear head (reduction ratio 4.1:1) for translational motion via a ball screw (1 mm lead) and the other with a built-in gear head (reduction ratio 67:1) for pivoting.

The strokes of the plate modules for the index and middle fingers are both 57 mm. The stroke of the plate module for the thumb is 114 mm and the rotation range for pivoting is ±35°.

The total weight of the prototype (including motors but excluding driver circuits) is approximately 5 kg.

5.4. Discussion

In this section, we discuss the remaining problems and some issues to be argued. One of the remaining problems is motion planning of the designed device attached to the base module. We are now considering a motion-planning algorithm to locate each surface patch at the expected contact point based on the tracking data of human fingers (Yokokohji et al. 2004). To develop the motion-planning algorithm, we must measure the approaching and pre-shaping behaviors of a human in a grasping task. We should also consider how to measure finger motion when simulating the object grasping, since we want to keep the user's hand bare and avoid using a data-Glove-like sensing device if possible.

One might argue whether the designed mechanism is a unique solution. Of course, type B is not the only mechanism corresponding to the contact profile shown in Figure 11. Compared to other possibilities, we concluded that type B is a reasonable solution. We must also keep in mind that there might be other good reference frames from which one can inspire better mechanisms than type B. Since the motion-planning

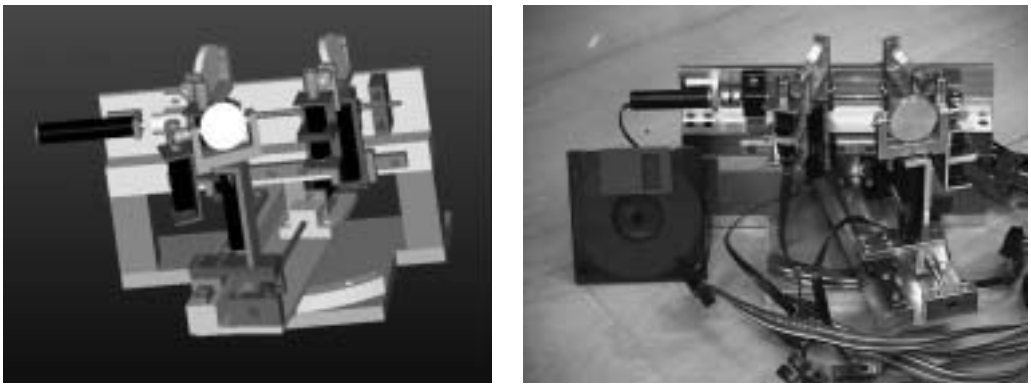

(a) (b)

Fig. 15. Prototyped contact module: (a) CAD model; (b) prototype (with a floppy disk).

algorithm depends on the mechanism of the contact module, we should also consider the mechanism so that it makes the motion-planning algorithm simple.

One might also argue whether the flat surface patches are enough. Actually, the shape of the surface patch is a remaining issue. As shown in Figure 14(a), we simply adopted a flat circular plate. When a user is trying to grasp a cylinder, it would be ideal if the surface patches are rounded so that they can approximate the lateral face of the cylinder. We expect that the user could be convinced even with a flat surface patch if a virtual cylinder is visually displayed to the user because visual stimuli are dominant over haptic stimuli (well known as "visual capture"; Welch and Warren 1980). However, the user may not be fooled by a flat surface patch when his finger contacts the sharp edge of a virtual object. A small shape approximation device (Tachi et al. 1994, 1995) at each plate module may extend the range of objects that can be displayed by this device, but we must consider the trade-off between design complexity and versatility.

One might further argue whether the circular shape with a 30 mm diameter is the best shape and size of surface patch even if we accept the flat surface. To simulate grasping a very small object, the size of the surface patch should be small accordingly. Ideally, the size of surface patch could be as small as the contact area at the fingertips. However, the surface patch should be large enough to cover the tracking/prediction errors of the fingertip motions. There might be better shapes for the surface patch rather than just the circular shape to accommodate these contradicting requirements.

One might finally argue whether this kind of device can simulate elastic objects as well as rigid objects. When designing the device shown in Figure 15, we assumed simulating rigid objects only. This is why we used worm gears and ball screws, which are non-backdrivable or difficult to backdrive. If we could implement impedance control to each surface patch motion, it would be possible to simulate elastic objects. In such cases, however, we should make the surface patch backdrivable or implement a force sensor to each surface patch.

6. Simulation of Grasping Tasks

Since we have not established the motion-planning algorithm yet, we will just show the capability of the developed device itself without mounting on the base module. We selected three different objects: a tennis ball, a baseball bat, and a paint can. We first observed how the human grasps these objects and determined the locations of each surface patch. We implemented a simple PD-based servo loop on each joint of the device and tried to grasp the device just like the real objects.

Figures 16–18 show some photographs of the simulations as well as the case of grasping real objects. The tennis ball is an example of a small object that the current device can display. Note that the two surface patches for the index and middle fingers almost collide in this case. The baseball bat was selected as an example of an object which is larger than the device itself. As mentioned, the device can simply display local surface patches for the fingertips no matter how big the simulated object is. The paint can is an example of a large object that a human can grasp with one hand. Note that the orientation of the three surface patches becomes vertical in this case, whereas in the previous two cases the surface patches were slightly slanted in order to approximate the local contact areas.

7. Conclusion

In this paper, we have designed an encountered-type haptic display for multiple fingertip contacts to simulate the task of grasping an object of any shape and size. Before designing the device, we intensively observed human grasping behaviors. This observation was very helpful to determine the

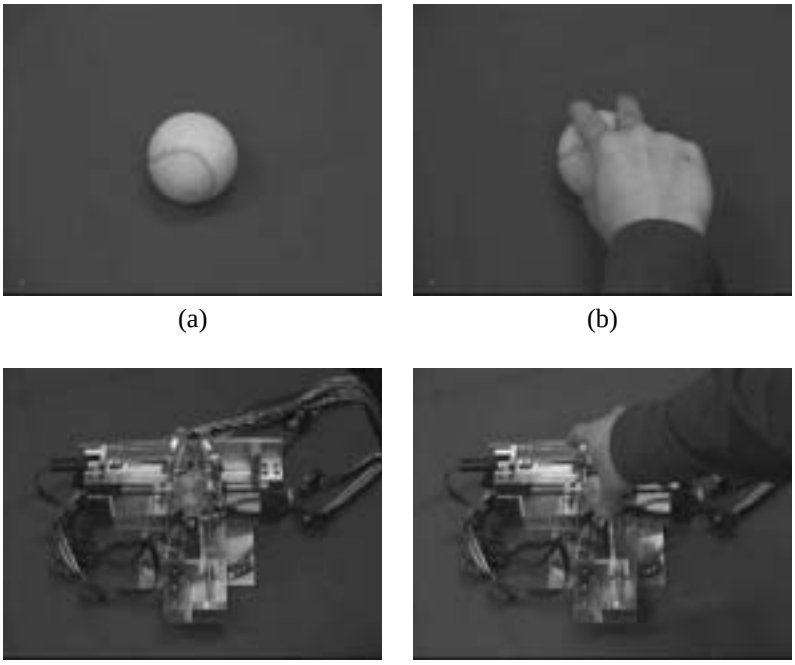

(a) (b)

(c) (d)

Fig. 16. Tennis ball: (a) real ball; (b) real ball grasped; (c) virtual ball; (d) virtual ball grasped.

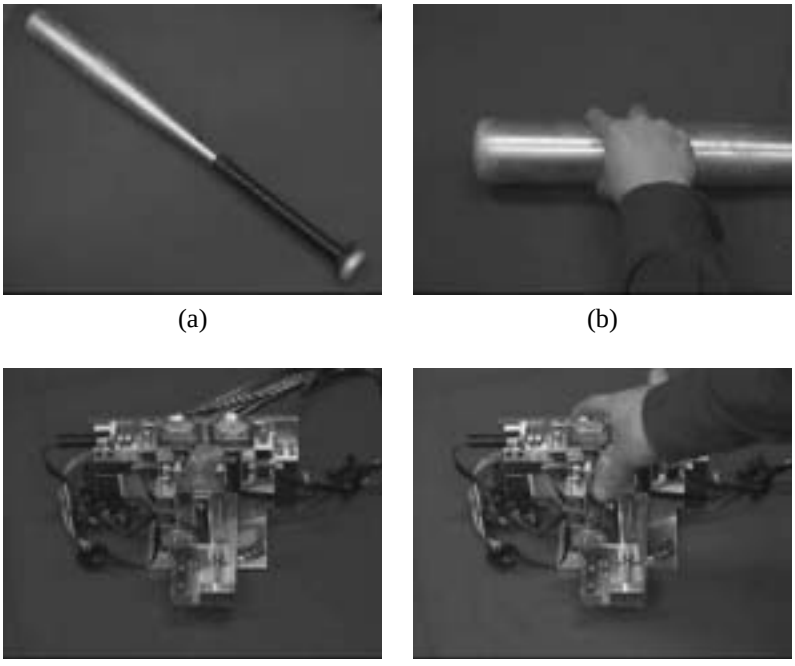

(a) (b)

(c) (d)

Fig. 17. Baseball bat: (a) real bat; (b) real bat grasped; (c) virtual bat; (d) virtual bat grasped.

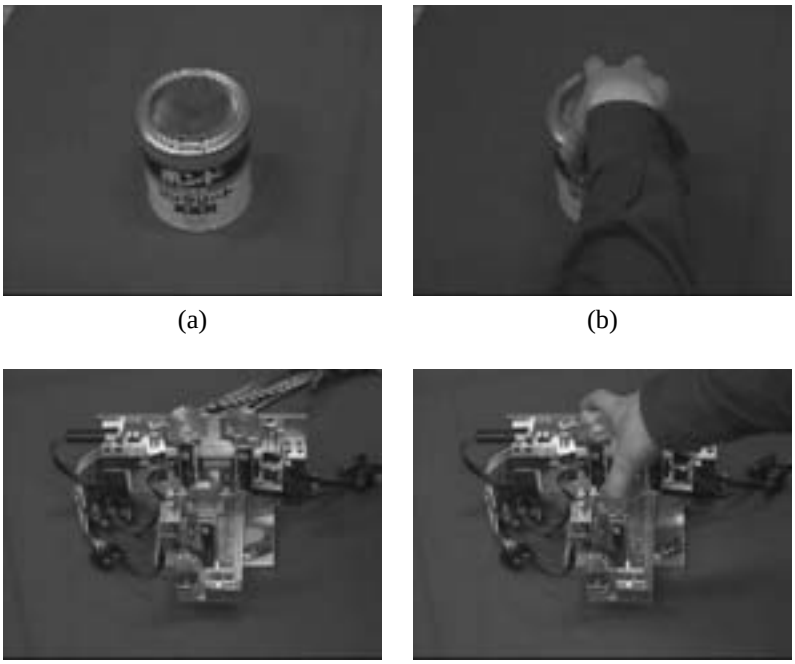

(a) (b)

(c) (d)

Fig. 18. Paint can: (a) real can; (b) real can grasped; (c) virtual can; (d) virtual can grasped.

mechanism of the device. In a sense, we just took the right way of designing, making the specification clear first and realizing this specification with a mechanism as simple as possible. In the robotics community, however, we tend to forget this basic philosophy (Bicchi 2000).

Based on our design, we have already prototyped a device. The potential capability of the developed device was shown by a preliminary experiment simulating different kinds of objects.

References

Barbagli, F., Salisbury, K. Jr., and Devengenzo, R. 2003. Enabling multifinger, multihand virtualized grasping. *Proceedings of the IEEE International Conference on Robotics and Automation (ICRA)*, Taipei, Taiwan, September 14–19, pp. 809–815.

Bicchi, A. 2000. Hands for dextrous manipulation and robust grasping: a difficult road towards simplicity. *IEEE Transactions on Robotics and Automation* 16(6):652–662.

Burstedt, M. K. O., Flanagan, J. R., and Johansson, R. S. 1999. Control of grasp stability in humans under different frictional conditions during multidigit manipulation. *Journal of Neurophysiology* 81:1706–1717.

Cutkosky, M. R. 1989. On grasp choice, grasp models, and the design of hands for manufacturing tasks. *IEEE Transactions on Robotics and Automation* 5(3):269–279.

Gruenbaum, P. E. et al. 1997. Implementation of dynamic robotic graphics for a virtual control panel. *PRESENCE* 6(1):118–126.

Hirota, K. and Hirose, M. 1993. Development of surface display. *Proceedings of the 1993 IEEE Virtual Reality Annual International Symposium (VRAIS'93)*, Seattle, WA, September, pp. 256–262.

Hirota, K. and Hirose, M. 1995. Simulation and presentation of curved surface in virtual reality environment through surface display. *Proceedings of the 1995 IEEE Virtual Reality Annual International Symposium (VRAIS'95)*, Research Triangle Park, NC, March, pp. 211–216.

Hirota, K. and Hirose, M. 1998. Implementation of partial surface display. *PRESENCE* 7(6):638–649.

Hoshino, H., Maeda, T., and Tachi, S. 1997. Virtual haptic space (X) – a system which enables an operator to touch a virtual object with two fingers. *Proceedings of the 2nd Annual Conference of the Virtual Reality Society of Japan*, Nagoya, Japan, pp. 17–18 (in Japanese).

Ikeuchi, K. and Suehiro, T. 1994. Toward an assembly plan from observation. i. task recognition with polyhedral objects. *IEEE Transactions on Robotics and Automation* 10(3):368–385.

Iwata, H., Yano, H., and Nakaizumi, F. 2001. Gait Master: a versatile locomotion interface for uneven virtual terrain. *Proceedings of IEEE Virtual Reality 2001*, Yokohama, Japan, pp. 131–137.

Jenmalm, P. 2000. Dextrous Manipulation in Humans: Use of Visual and Tactile Information about Object Shape in Control of Fingertip Actions. Ph.D. Dissertation, the Department of Integrative Medical Biology, Umeå University.

Jenmalm, P., Goodwin, A. W., and Johansson, R. S. 1998. Control of grasp stability when humans lift objects with different surface curvatures. *Journal of Neurophysiology* 79:1643–1652.

Johansson, R. S., Westling, G., Bäckström, A., and Flangan, J. R. 2001. Eye–hand coordination in object manipulation. *Journal of Neuroscience* 21:6917–6932.

Kaneko, M., Tanaka, Y., and Tsuji, T. 1996. Scale-dependent grasp: a case study. *Proceedings of the IEEE International Conference on Robotics and Automation (ICRA)*, Minneapolis, MN, pp. 2131–2136.

Kaneko, M., Tanaka, Y., and Tsuji, T. 1997. On three phases for achieving enveloping grasps—inspired by human grasping. *Proceedings of the IEEE International Conference on Robotics and Automation (ICRA)*, Albuquerque, NM, pp. 385–390.

Kapandji, I. A. 1982. *Physiology of the Joints (Upper Limbs)*, Elsevier Science, Amsterdam.

Kawasaki, H., Takai, J., Tanaka, Y., Mrad, C., and Mouri, T. 2004. Control of multifingered haptic interface opposite to human hand. *Proceedings of the IEEE/RSJ International Conference on Intelligent Robots and Systems (IROS)*, Sendai, Japan, September 28–October 2, pp. 2707–2712.

Kuniyoshi, Y., Inaba, M., and Inoue, H. 1994. Learning by watching: extracting reusable task knowledge from visual observation of human performance. *IEEE Transactions on Robotics and Automation* 10(6):799–822.

McNeely, W. A. 1993. Robotic graphics: a new approach to force feedback for virtual reality. *Proceedings of the 1993 IEEE Virtual Reality Annual International Symposium (VRAIS'93)*, Seattle, WA, September, pp. 336–341.

Napier, J. 1997. The prehensile movements of the human hand. *Journal of Bone Joint Surgery* 38B(4):902–913.

Saito, F. and Nagata, K. 1999. Interpretation of grasp and manipulation based on grasping surfaces. *Proceedings of the IEEE International Conference on Robotics and Automation (ICRA)*, Detroit, MI, pp. 1247–1254.

Saito, F. and Nagata, K. 2001. Description of grasp and manipulation and design of robot hands. Journal of the Robotics Society of Japan 19(3):333–344 (in Japanese).

Tachi, S. et al. 1994. A construction method of virtual haptic space. *Proceedings of the International Conference on Artificial Reality and Telepresence (ICAT'94)*, Tokyo, Japan, July, pp. 131–138.

Tachi, S. et al. 1995. A machine that generates virtual haptic space. *Video Proceedings of the Virtual Reality Annual International Symposium (VRAIS'95)*, Research Triangle Park, NC, March.

Welch, R. B. and Warren, D. H. 1980. Immediate perceptual response to intersensory discrepancy. *Psychological Bulletin* 88(3):638–667.

Yokokohji, Y., Hollis, R. L., and Kanade, T. 1999. WYSIWYF display: a visual/haptic interface to virtual environment. *PRESENCE* 8(4):412–434.

Yokokohji, Y., Kinoshita, J., and Yoshikawa, T. 2001. Path planning for encountered-type haptic devices that render multiple objects in 3D space. *Proceedings of IEEE Virtual Reality 2001*, Yokohama, Japan, pp. 271–278.

Yokokohji, Y., Muramori, N., Sato, Y., Kikura, T., and Yoshikawa, T. 2004. Design and path planning of an encountered-type haptic display for multiple fingertip contacts based on the observation of human grasping behavior. *Proceedings of the IEEE International Conference on Robotics and Automation (ICRA)*, New Orleans, LA.

Yoshikawa, T. and Nagura, A. 2001. A touch/force display system for haptic interface. *PRESENCE* 10(2):225–235.

Yoshikawa, T. and Yoshimoto, K. 2000. Haptic simulation of assembly operation in virtual environment. *Proceedings of the ASME, Dynamic Systems and Control Division*, Orlando, FL, pp. 1191–1198.